Effect of thermal cycling heated Fibre Metal Laminates under static load

Hagenbeek, Michiel; Sinke, Jos

DOI
10.1016/j.compstruct.2018.12.042

Publication date
2019

Document Version
Accepted author manuscript

Published in
Composite Structures

Effect of thermal cycling heated Fibre Metal Laminates under static load

Michiel Hagenbeek*, Jos Sinke

Structural Integrity & Composites, Faculty of Aerospace Engineering, Delft University of Technology, Kluyverweg 1, 2629 HS Delft, The Netherlands

Abstract

Heated GLARE, a Fibre Metal Laminate with an integrated heater element, has been developed for de- or anti-icing systems in aircraft structures. Besides cyclic thermal loading these structures are also subjected to mechanical loading. To investigate the effect of static loading in addition to thermal cycling a series of tests have been performed on heated GLARE using a specifically designed mechanical load fixture and thermal cycling setup. Three different tensile stress levels, 150, 200 and 300 MPa, were used in combination with up to 36,000 thermal cycles between -20 and 50 °C.

The effect of the combined thermo-mechanical loading was investigated by testing the interlaminar shear properties of each sample after thermal cycling. Thermal cycling under a 150 MPa static load showed much less reduction or even increase in strength compared to previously reported test results for thermal cycling only. This effect was not found for thermal cycling under the 200 and 300 MPa static load cases. On the contrary, in these cases more reduction in strength was found compared to test results after thermal cycling without static load.

Keywords: Glass-fibre epoxy composite, heated GLARE, thermal cycling, prestress, interlaminar shear strength

*Corresponding author
Email address: m.hagenbeek@tudelft.nl (Michiel Hagenbeek)
URL: www.tudelft.nl/ae (Michiel Hagenbeek)

1. Introduction

Leading edges have to be heated occasionally to avoid atmospheric ice accumulation on the surface of the wings. Ice accumulation can alter the shape of the air foil and lead to loss of aerodynamic performance. In Fibre Metal Laminates, such as GLARE, an electrical heater element can be integrated in the layup. This so called heated GLARE is subjected to a combination of thermal loading and mechanical loading during the aircraft service life. In addition, moisture absorption can influence the durability of the material.

In previously reported research the effect of thermal cycling and moisture on heated GLARE has been examined separately and in combination with each other [1, 2, 3]. The effect of additional static loading was however not yet considered in these investigations. Long term cycling up to 144,000 cycles was performed to approximate the expected total number of thermal cycles of a potential heated GLARE deicing system over the aircraft service life. In all reported test results the maximum decrease in interlaminar shear strength (ILSS) after thermal cycling was found in the first stage from 0 to 10,000 cycles (-32.9% for heated GLARE cycled between -20 and 50 °C). This initial drop in strength was followed by a recovery phase and a resumed decline after roughly 60,000 cycles [3]. No crack or voids or other visible changes were found in the optical microscope images and the drop is expected to be caused by internal stress relief. This confirmed the initial investigation of Graafmans on GLARE3 edges subjected to 986 thermal cycles between -50 and 80 °C on GLARE3 in which no sign of delamination, debonding or cracks at the specimen edges was found either [4].

In flight the wing leading edge is not only subjected to thermal loading, as a result of deicing and flight conditions, but also to mechanical loading. The combination of mechanical fatigue, elevated temperature and moisture exposure has been addressed for GLARE and aluminium 2024-T3 in the literature. The aluminium 2024-T3 crack growth is unaffected by elevated temperature (70 °C) according to Rans [5] and Homan [6, 7]. While an increase in crack growth re-

sistance was exhibited at lower temperatures. Experiments performed on Glare 3-3/2-0.3 by Homan [8] showed that 3000 hour exposure to high temperature (70 °C) and humidity (85%RH) prior to testing has no effect on the fatigue initiation. Ypma reports that combined temperature and moisture exposure lead to higher crack growth rates, especially if exposure is intermittent and not only prior to fatigue testing [9]. The crack bridging is then less effective. An increase in temperature causes an increase in crack growth as well [10]. Whereas temperatures below 0 °C postpone the crack initiation time and decrease the crack propagation rate considerably [11]. The influence of temperature on crack growth behaviour in the metal layers, delamination growth between the metal and fibre layers, and residual stresses within the fibre metal laminate has been studied by Rans and Alderliesten as well [5]. The crack growth rate at 70 °C was higher than at 20 °C due to the reduced delamination growth resistance at elevated temperature. The crack growth rate of aged specimens are however still far less than the crack growth rates in aluminium.

The combination of both mechanical and thermal fatigue is mentioned by Broest and Beumler using dedicated thermal cycling setups in both cases. Broest investigated fatigue crack initiation of GLARE door corner specimens after 40,000 pre-fatigue cycles and 20,000 additional load spectra (which represented 20,000 flights) under a -30 to 20 °C thermal cycling regime (120 s for each flight cycle) [12]. No crack initiation occurred at the inspected side after these loadings. Beumler calculated the crack initiation life accounting for the additional thermal stresses each flight due to different thermal expansion coefficients of the GLARE constituents and thermal cycling (-30 °C to +70 °C). He found a 50% decrease in crack initiation life compared to calculated result under constant temperature (20 °C). However, the improved crack growth behaviour of aluminium 2024-T3 at temperatures below 0 °C and the load redistribution from the aluminium to the fibres due to the stiffer resin at low temperatures compensates the calculated disadvantage [11]. Li showed that 1,000 thermal cycles between -65 to +135 °C hardly changed the fatigue crack growth in a novel fibre metal laminate based on an aluminium-lithium alloy and S4-glass

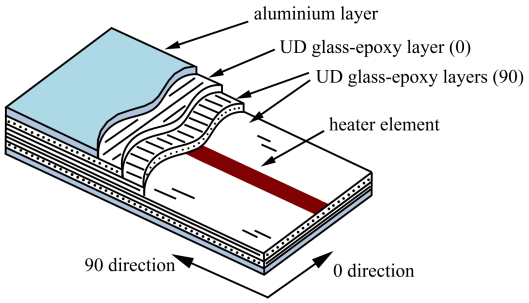

Figure 1: Schematic lay-up of a heated GLARE laminate.

polysulfone-epoxy prepreg [13].

The effect of combined static mechanical loading and cyclic thermal loading has hardly been addressed in literature. In the current paper the effect of a static tensile load in addition to thermal cycling on heated GLARE will therefore be investigated. The question to be answered is if a static tensile load will affect the observed change in ILSS, especially the drop in strength in the initial thermal cycling stage up to 10,000 cycles. To simulate the influence of thermal fatigue under a tensile load Graafmans prestrained GLARE3-3/2-0.2 with 0.6% permanent elongation. Special GLARE2 and GLARE3 laminates with 2.6mm thick layers of aluminium were used to increase the compressive stress to 149 MPa on the prepreg in fibre direction. The specimens were subjected to 986 thermal cycles between 50 °C and 80 °C and did not show any failure. To be able to assess higher amount of cycles and higher stress levels another approach is needed, which will be detailed hereafter.

2. Heated GLARE

2.1. The heated GLARE lay-up

In the current research a GLARE5B-2/1-0.3 layup is used, which is build up from 4 unidirectional (UD) glass-fibre epoxy layers in both 0°and 90°direction and 0.3 mm thick aluminium sheets [14]. A schematic lay-up of such a heated GLARE laminate is depicted in Figure 1. The heating function is introduced by

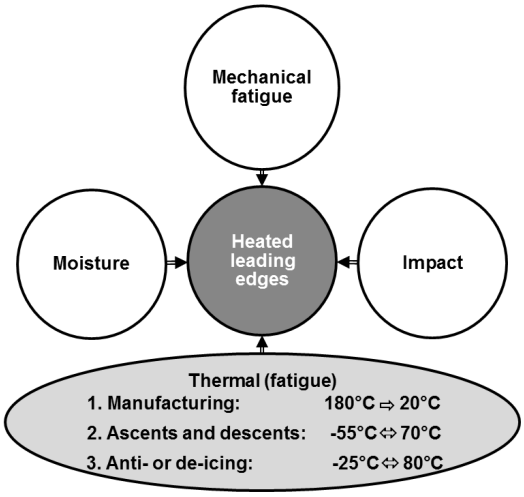

Figure 2: Major loading conditions of heated leading edges made of heated GLARE.

embedding a thin copper heater element along the 90° direction between both central 90° UD glass-fibre epoxy layers. By integrating a heating functionality in the structural aircraft material GLARE the material can potentially be applied for de-/anti-icing of aircraft leading edges [13].

Instead of FM94 prepreg, used for conventional GLARE, FM906 glass-fibre epoxy prepreg is used in heated GLARE laminates. For FM94 the stiffness significantly decreases at temperatures beyond 70 °C [17]. The FM906 prepreg has higher glass transition (Tg = 135 °C vs. 103 °C) and curing (180 °C vs. 120 °C) temperature than FM94 prepreg and this results in a higher allowable service temperature of 120 °C [15]. Similar to conventional GLARE, heated GLARE is autoclave cured in one hour at 6 bars of pressure [16]. The vacuum, pressure and temperature set points which are used for manufacturing of heated GLARE can be found in already reported research [1].

2.2. Leading edge loading conditions

The major loading conditions for heated leading edges are given in Figure 2. The heated leading edges are subjected to both mechanical and thermal loading. Mechanical stresses in the material develop due to the aerodynamic and

gravitational loading of the wing. Different thermal expansion coefficients of the heated GLARE constituents (aluminium, epoxy, glass-fibre, copper) lead to thermal stresses in the material after manufacturing. These thermal stresses change continuously as a result of temperature changes during ascents and descents (once per flight) [16] and due to internal heating in case of anti- and de-icing (several times per flight) [18, 19, 20].

Therefore, both the mechanical and the thermal loading have a cyclic nature and can lead amongst others to fatigue damage [21]. Moreover, the elevated temperatures in case of anti- and de-icing are expected to cause physical ageing of the epoxy [2, 22]. Damage on the leading edge can also be caused by impact, for example due to bird strike, and more gradually due to moisture ingress during the lifetime of the structure.

3. Experimental procedures

3.1. Thermal cycling setup

A dedicated thermal cycling setup was build and used to perform thermal cycling tests under a static load. The setup is shown in Figure 3. The tensile load is applied on the test sample by a lever system and a dead weight. The dead weight consists of a selection of lead blocks with the required total mass. A strain gauge on the sample is used to verify the applied load on the sample. Internal heating of the sample is achieved by resistance heating of a copper heater element connected to a power supply. This working principle is similar to the intended use as anti-/de-icing system.

For external cooling of the sample Peltier elements are used in stacks of two on both sides, with small fans on top of the hot side of the Peltier elements to loose the excess of heat. The cooling capability is enhanced by placing the whole setup in a climate chamber at -25 °C. The thermal cycling is computer controlled using embedded thermocouples. The system switches between heating and cooling and vice versa when predefined temperatures are reached. By

adapting the heating and cooling power the temperature range and profile can be easily adapted.

3.2. Thermal cycling samples

In total six specially designed heated GLARE 5-2/1-0.3 samples were investigated in this study. The sample dimensions and arrangement are given in Figure 4. The samples consist of two 0.3 mm thick aluminium layers, four glass fibre-epoxy layers with fibre orientations [0/90/90/0] and a 0.03 mm thick and 5.0 mm wide embedded copper heater element at the centre. The thermal and mechanical loading conditions of the test samples are given in Table 1.

Sample TM-HGL0 was not thermal cycled but used as a reference. All other samples were thermal cycled from -20 to 50 °C. Two thermocouples (TC1, TC2) were embedded in the samples to monitor and control the thermal loading. The thermocouples were placed on top of the heater element with a single glass-fibre epoxy layer in between. The in-plane positions of the thermocouples are depicted in Figure 4.

Table 1: Samples: Nomenclature (nom), materials, thermal loading conditions and number of cycles (noc).

nom	T_{min} [°C]	T_{max} [°C]	Stress level [MPa]	noc [-]
Heated GLARE				
TM-HGL0	na	na	-	0
TM-HGL1	-20	50	150	13,788
TM-HGL2	-20	50	150	24,000
TM-HGL3	-20	50	150	36,000
TM-HGL4	-20	50	200	27,769
TM-HGL5	-20	50	300	27,769

The heater element is positioned at the mid-plane in the 90°direction. The heater element is thereby stacked between two 90°glass-fibre epoxy layers with

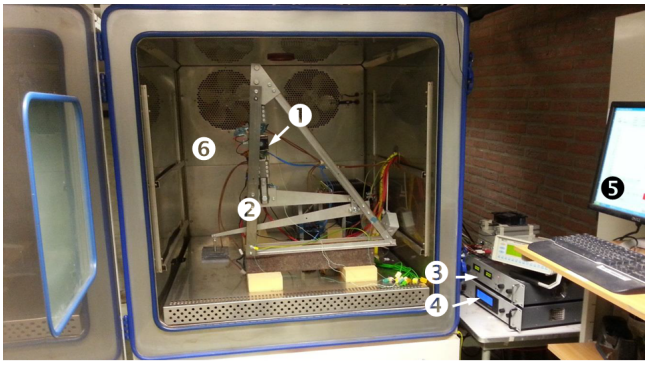

❶ Thermal cycling core & sample
❷ Loading fixture with levers
❸ Power supply 1
❹ Power supply 2
❺ Computer
❻ Climate chamber

(a)

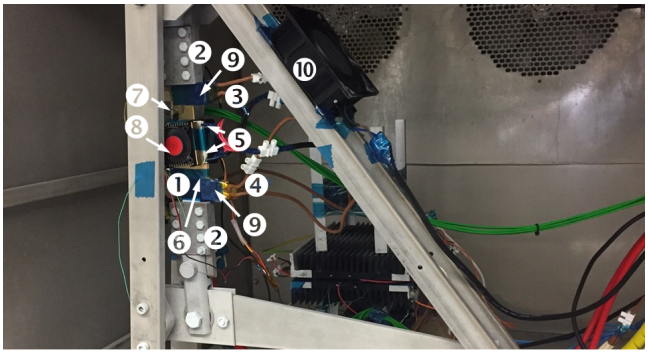

❶ Sample
❷ Loading clamps
❸ Electrical input
❹ Electrical output
❺ Peltier elements
❻ Embedded thermocouples
❼ Strain gage
❽ Heat sinks & fans
❾ Copper sample connectors
❿ Ventilator

(b)

Figure 3: The thermal cycling machine in the climate chamber (a) overview and (b) detail.

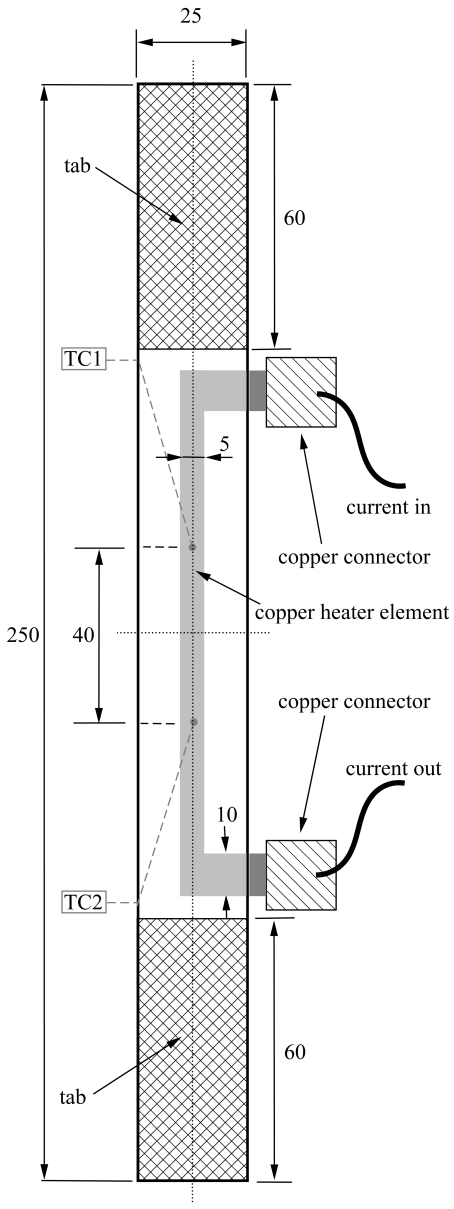

Figure 4: Sample dimensions and arrangement.

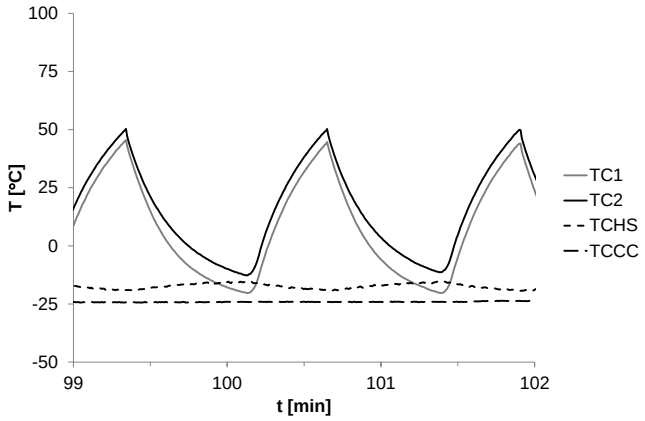

Figure 5: Typical thermal cycle for heated GLARE samples with climate chamber (CC) and heat sink (HS) temperatures.

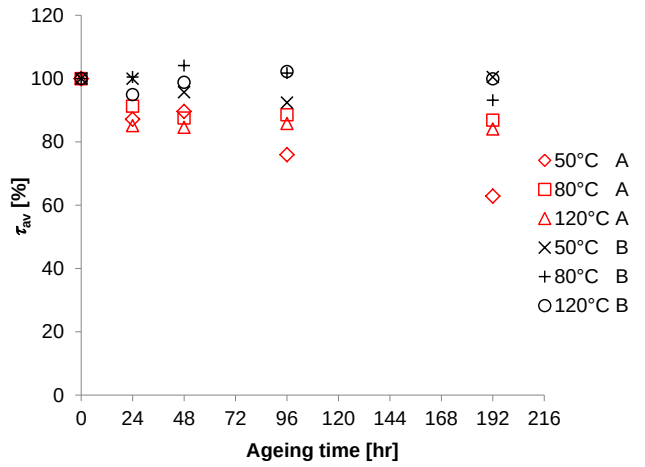

Figure 6: Overview of continuous heating tests showing the effect of thermal ageing on heated GLARE [2]. The interlaminar shear test specimens were taken at the position of the heater element (A) and next to the heater element (B).

the orientation along the fibre direction. The stiffness difference between the copper heater element and the glass-fibre epoxy layer is thereby reduced as much as possible in this direction.

Table 2: Total exposure time in hours after 12,000 thermal cycles for heated GLARE under static loading (cf. Figure 5) and heated GLARE without static loading [3].

Temp. range [°C]	TM-HGL1 [h]	HGL16 [h]
-30 to -20	0.0	0.0
-20 to -10	85.0	28.3
-10 to 0	39.0	15.0
0 to 10	29.0	11.7
10 to 20	27.0	10.0
20 to 30	27.0	6.7
30 to 40	29.0	7.5
40 to 50	17.0	9.2
50 to 60	0.0	0.0
60 to 70	0.0	0.0
70 to 80	0.0	0.0
80 to 90	0.0	0.0
90 to 100	0.0	0.0
Σ	253.0	88.3
Min temp [°C]	-20	-20
Max temp [°C]	50	50
Cycle time [s]	75.9	26.5
Max cycles [kC]	36	144
Total time [days]	31.6	44.2

3.3. Thermal cyclic fatigue testing

The temperature range in the thermal cycling tests was chosen from -20 to 50 °C. The typical thermal cycles for the heated GLARE 5-2/1-0.3 samples are

shown in Figure 5. Thermal cycling tests in this temperature range showed the largest decrease in ILSS in previous research [2, 3]. In this range the negative effect of internal stress relief on the ILSS is not counteracted by the positive ageing effect on the glass-fibre epoxy as present at higher temperatures. In continuous heating tests performed on heated GLARE in previous research the effect of the maximum temperature on the ILSS can be clearly seen for specimens taken at the heater element (Figure 6) [2].

In Table 2 the total exposure time in hours after 12,000 thermal cycles is given for the heated GLARE samples under static loading. The cycle time, minimum and maximum temperature, maximum number of cycles, and the total time are given as well. For comparison the total exposure time for a heated GLARE sample without static loading (HGL16), as reported in previous research, is listed in the same table [3]. From this table it can be seen that the cycle time for heated GLARE samples is almost three times longer than in the previously reported research. This is caused by the much less cooling capacity. The chosen heat sinks and fans needed to be small due to limited space between the sample and the fixture.

3.4. Interlaminar shear strength testing

The effect of the thermo-mechanical loading was investigated by testing the interlaminar shear properties of each sample after cycling. The ILSS tests were performed in fourfold on all samples listed in Table 1 according to the ASTM standard [23]. The mean values have been determined for each set of data and are given together with the scatter (absolute minimum and maximum values) in the resulting graphs. The specimens have a width of 4 mm and a length of 20 mm. The ILSS tests were conducted on a 25 kN test machine with a test speed of 1 mm/min. Correct failure modes were obtained in all tests.

Figure 7 shows the ILSS results for the heated GLARE specimens TM-HGL1 to TM-HGL3 thermal cycled between -20 and 50 °C under a 150 MPa static loading. The ILSS specimens were taken at the location of the heater element (position A) and both the absolute values and the comparison with the

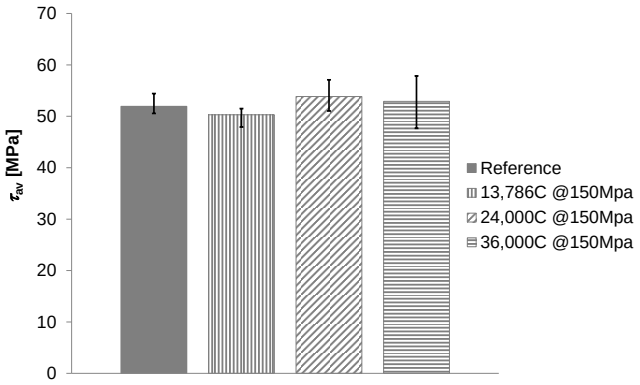

(a)

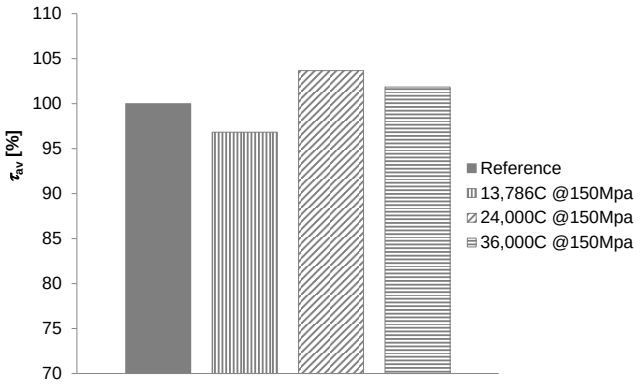

(b)

Figure 7: Heated GLARE specimens TM-HGL1 to TM-HGL3 (150 MPa loading) taken from position A (at the heater element) : (a) absolute ILSS values and (b) comparison with the (non-cycled) reference (cf. Table 1).

non-cycled (and non-loaded) reference TM-HGL0 are given. In Figure 8 the ILSS results are given for the ILSS specimens taken next to the heater element (position B).

In Figure 9 the ILSS results are given for the heated GLARE specimens TM-HGL1 to TM-HGL3 thermal cycled between -20 and 50 °C under 200 MPa and 300 MPa static loading respectively. The ILSS specimens were taken at the location of the heater element (position A) and both the absolute values and the comparison with the non-cycled reference TM-HGL0 are given.

4. Results and discussion

With a 150 MPa static load a maximum -3.6% reduction in ILSS after 13,786 was found compared to the non-cycled reference and after 36,000 cycles a +7.1% increased value was found for specimens taken from position A at the heater element (see Figure 7). Similar to the results found by Graafmans, the specimens did not show any failure [4]. The ILSS values for specimens taken from the position next to the heater element show a slight increase compared to the non-cycled reference (see Figure 8). this is expected to be caused by physical ageing and in line with previosly reported results [2]. Thermal cycling tests without mechanical loading in previous research showed -10.8% decrease after 12,000 cycles, -13.8% after 24,000 cycles and -14.4% after 36,000 cycles in the same temperature range of -20 to 50 °C as a result of internal stress relief [3]. The 150 MPa static load is expected to prevent this internal stress relief due to thermal cycling and thus less reduction is found.

The ILSS for the thermal cycled samples with 200 MPa and 300 MPa static load on the contrary show a large decrease as seen in Figure 9. In this case the decrease is actually much larger than previously found ILSS results for heated GLARE after thermal cycling only as listed above. The largest decrease in strength, -25.7% compared to the non-cycled reference, was found for the sample with 300 MPa static load and 27,769 thermal cycles. The 200 MPa and 300 MPa load cases not only result in much higher internal stresses compared

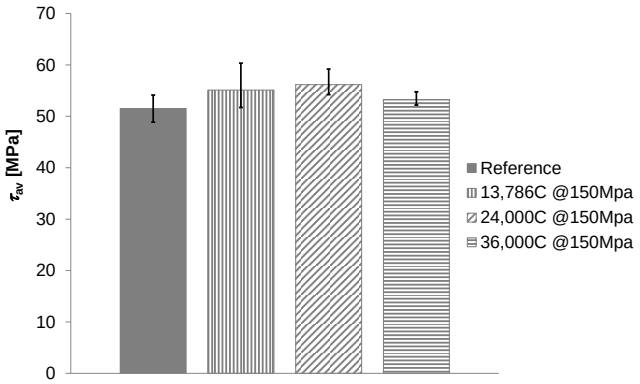

(a)

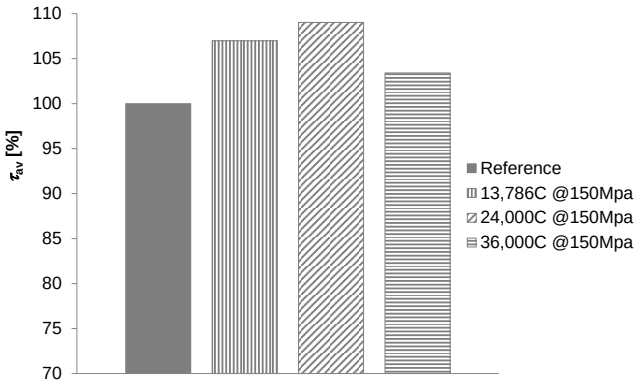

(b)

Figure 8: Heated GLARE specimens TM-HGL1 to TM-HGL3 (150 MPa loading) taken from position B (next to the heater element): (a) absolute ILSS values and (b) comparison with the (non-cycled)reference (cf. Table 1) .

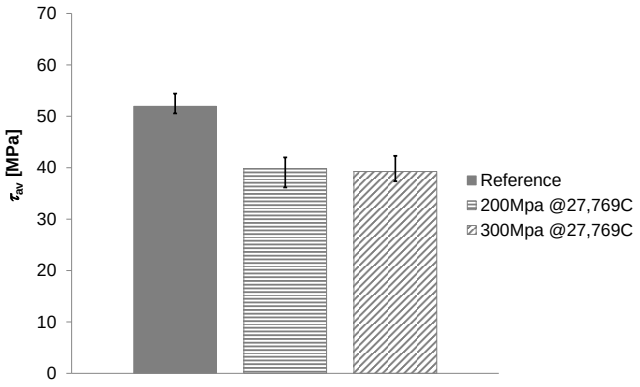

(a)

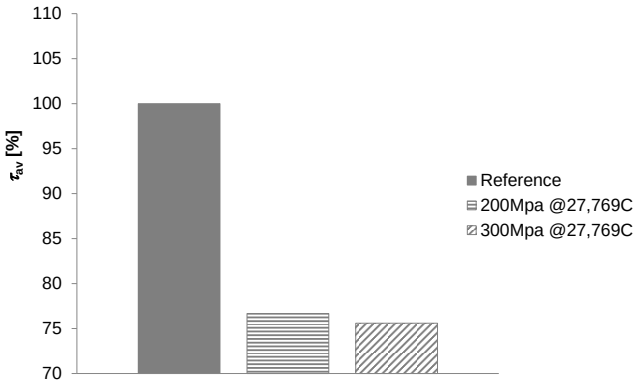

(b)

Figure 9: Heated GLARE specimens TM-HGL4 & TM-HGL5 (200 MPa and 300 MPa loading resp.) taken from position A (at the heater element): (a) absolute ILSS values and (b) comparison with the (non-cycled) reference (cf. Table 1).

to the 150 MPa load case, but also lead to plasticity in the aluminium layers (as indicated by calculations based on Classical Laminate Theory) and thus a permanent change in internal stress distribution. These factors in combination with internal stress relief due to thermal cycling are expected to cause the larger reduction in ILSS here.

5. Conclusions

The specifically designed mechanical load fixture and thermal cycling setup enable thermal cycling tests under a static load. Heated GLARE, a Fibre Metal Laminate with an integrated heater element, was thermo-mechanically tested at three different tensile stress levels, 150, 200 and 300 MPa, in combination with up to 36,000 thermal cycles between -20 and 50 °C. The effect of the combined thermo-mechanical loading was investigated by measuring the interlaminar shear properties of each sample.

With a 150 MPa static load a maximum reduction of -3.6% in ILSS after 13,786 was found compared to the non-cycled reference and for 36,000 cycles even a +7.1% increased value was found. These values are considerably higher than previously reported for thermal cycling only and indicate a positive effect of the additional static load. This positive effect is however not present at the higher stress values (200 and 300 MPa), which on the contrary show larger decreases in ILSS compared to results after thermal cycling only. The largest decrease in strength was found for the sample with 300 MPa static load and 27,769 thermal cycles: -25.7% compared to the non-cycled reference. The more pronounced reduction in ILSS is expected to be caused by a combination of higher internal stresses, a permanent change in internal stress distribution as a result of plasticity in the aluminium layers, and internal stress relief due to thermal cycling.

Thus, the addition of a static load has a distinct influence on the interlaminar shear properties after thermal cycling and the chosen stress level determines if the effect is positive or negative.

6. Acknowledgements

This study is funded by the Dutch Technology Foundation STW and Fokker Aerostructures.

7. References

[1] Müller B, Hagenbeek M and Sinke J (2016) Thermal cycling of (heated) Fibre Metal Laminates. Composite Structures, 152, p.106-116.

[2] Hagenbeek M, Müller B, and Sinke J (2018) Effect of thermal cycling and ageing on heated Fibre Metal Laminates and glass-fibre epoxy composites. Advanced Engineering Materials, https://doi.org/10.1002/adem.201800084

[3] Hagenbeek M, and Sinke J (2018) Effect of long-term thermal cycling and moisture on heated Fibre Metal Laminates and glass-fibre epoxy composites. Composite Structures, 210, p.500-508.

[4] Graafmans G (1995) Thermal Behaviour of Fibre Metal Laminates, Master thesis, Delft University of Technology, Delft, The Netherlands.

[5] Rans C D and Alderliesten R C (2009) The Influence Of Temperature on Crack Growth in Fiber Metal Laminates. 12th International Conference on Fracture, Ottawa.

[6] Homan J J (2001) Crack growth properties of thin aluminium sheets. Report B2V-01-16, issue 2, Delft University of Technology, Delft, The Netherlands.

[7] Homan J J (2002) Crack growth properties of thin aluminium sheets at various temperatures. Report B2V-02-39, Delft University of Technology, Delft, The Netherlands.

[8] Homan J J (2006) Fatigue Initiation in Fibre Metal Laminates. International Journal of Fatigue, Vol. 28, No. 4, 2006, p.366-374.

[9] Ypma M S (2001) Overview of tests concerning the influence of temperature and environmental exposure on Glare. Report B2V-00-41, Glare Research Program, Delft.

[10] Borgonje B and Ypma M S (2003) Long term behaviour of Glare. Applied Composite Materials 10, p. 243-255.

[11] Beumler T (2004) Flying Glare, A contribution to aircraft certification issues on strength properties in non-damaged and fatigue damaged Glare structures. Ph.D. thesis, Delft University of Technology, Delft University Press, The Netherlands.

[12] Broest P (2002) Fatigue of door corners under flight-cycle loading. Report B2V-02-42, Delft University of Technology, Delft, The Netherlands.

[13] Li H, Hu Y, Liu C, Zheng X, Liu H and Tao J (2016) The effect of thermal fatigue on the mechanical properties of the novel fiber metal laminates based on aluminium-lithium alloy. Composites: Part A 84, p.36-42.

[14] Fibre Metal Laminates Centre of Competence, http://www.fmlc.nl, accessed 28.8.2018.

[15] Pacchione M and Telgkamp J (2006) Challenges of the metallic fuselage, Proceedings of the 25^{th} International congress of the aeronautical sciences (ICAS), p.1-12.

[16] Vermeeren C A J R, Beumler Th, De Kanter J L C G, Van der Jagt O C and Out B C L (2003) Glare Design Aspects and Philosophies, Applied Composite Materials 10, p.257-276.

[17] Hagenbeek M (2005) Characterisation of Fibre Metal Laminates under Thermo-mechanical Loadings, PhD thesis, Delft University of Technology, Delft, The Netherlands.

[18] Federal Aviation Administration (FAA) (2010), Airplane and Engine Certification Requirements in Supercooled Large Drop, Mixed Phase and Ice Crystal Icing Conditions, Federal Register 75 (124), 37311-37339.

[19] Mohseni M, and Amirfazli A (2013) A novel electro-thermal anti-icing system for fiber-reinforced polymer composite airfoils, Cold Regions Science and Technology, 87, p.47-58.

[20] Müller B, Anisimov A G, Sinke J and Groves R M (2015) Thermal strains in heated fibre metal laminates. Proc. of the 6^{th} Int. Con. on Emerging Technologies in Non-destructive Testing (ETNDT), p.1-6.

[21] Alderliesten R C (2017) Fatigue and Fracture of Fibre Metal Laminates. Solid Mechanics and Its Applications. Springer International Publishing. Vol. 236, DOI 10.1007/978-3-319-56227-8_1

[22] Odegard G M and Bandyopadhyay A (2011) Physical Aging of Epoxy Polymers and Their Composites. J. of Polymer Science Part B: Polymer Physics, 49 (24), p.1695-1716.

[23] ASTM, Standard Test Method for Short-Beam Strength of Polymer Matrix Composite Materials and Their Laminates, ASTM standards, D2344/D2344M-13.